Mantle convection models with viscoelastic/brittle lithosphere: Numerical methodology and plate tectonic modeling

Louis Moresi, Hans Mühlhaus, Frédéric Dufour

CSIRO Exploration and Mining, PO Box 437, Nedlands, WA 6009, Australia. (email: l.moresi@ned.dem.csiro.au, http://www.ned.dem.csiro.au/research/solidMech/ Fax: +61 89389 1906; Phone +61 8 9389 8421)

Abstract

The Earth's tectonic plates are strong, viscoelastic shells which make up the outermost part of a thermally convecting, predominantly viscous layer. In order to build a more realistic simulation of the planet's evolution, the complete viscoelastic convection system ought to be included. A particle-in-cell finite element method is demonstrated which can simulate very large deformation viscoelasticity. This is applied to a plate-deformation problem. Numerical accuracy is demonstrated relative to analytic benchmarks, and the characteristics of the method are discussed.

Introduction

Underneath the lithospheric plates of the Earth lies the mantle (Figure 1). Approximately 3000km deep, it is composed of solid rock that is warm enough to deform like a viscous fluid, albeit at speeds of a few centimetres per year. The plates move because the mantle is forever stirring as heat generated by natural radioactive decay struggles to escape via thermal convection. In the lithosphere the rocks are significantly cooler and behave as a viscoelastic, brittle solid. In regions of high stress, brittle failure gives rise to earthquakes.

This picture of the Earth's interior is widely accepted by geophysicists. It clearly indicates that the fundamental process is thermal convection; plate tectonics is the manner in which the system organizes. Therefore, a consistent model of plate behaviour should contain a description of the convection system of which the plate is a part. The principle difficulty for modeling is that plate tectonics is itself only a kinematic description of the observations: a fully consistent dynamic description of the motion of the plates is still sought.

There have been some major steps towards the simulation of plate tectonics in recent years by solving brittle/viscous fluid flow equations (e.g. Tackley 1998, 2000, Moresi & Solomatov, 1998 [1,2,3]). The importance of elasticity has not been quantified by such modeling. In the past, viscoelastic convection simulations have been limited to models with explicit layering in which a non-convecting viscoelastic layer is coupled to a viscous convecting domain (Podladchikov et al, 1993 [4]). Models of subduction zones which incorporate viscoelasticity, faulting, and free-surface behaviour have generally been limited to modest evolution times, after which further deformation produces severe remeshing problems (e.g. Melosh, 1978, Gurnis et al, 1996 [5,6]).

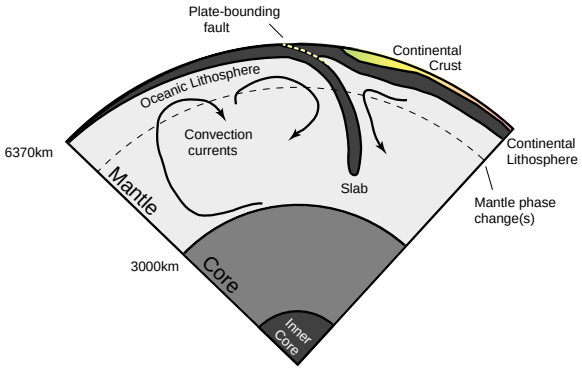

Figure 1: A simplified cross section of the Earth with major layerings shown to scale except for the upper boundary layer which is exaggerated in thickness by a factor of roughly two.

Having identified the need for efficient, large-scale convection simulations with elastic effects in an evolving cool lithosphere, we present a method for simulating viscoelastic-brittle materials in extreme deformation, and demonstrate its application.

Mathematical model

We begin our analysis in a general way with the classical momentuum conservation equation:

$$\nabla . \boldsymbol{\sigma} = \boldsymbol{f} \tag{1}$$

where $\boldsymbol{\sigma}$ is the stress tensor and $\boldsymbol{f}$ a force term. As we are interested only in very slow deformations of highly viscous materials, (infinite Prandlt number) we have neglected all intertial terms in (1). It is convenient to split the stress into a deviatoric part, $\boldsymbol{\tau}$, and an isotropic pressure, p,

$$\boldsymbol{\sigma} = \boldsymbol{\tau} - p\mathbf{I} \tag{2}$$

where $\boldsymbol{I}$ is the identity tensor.

Viscoelasticity

We will employ a Maxwell viscoelastic model which has been used in previous studies of lithospheric deformation where viscous and elastic effects are important such as post-glacial rebound (Peltier, 1974 [7]). This model assumes that the strain rate tensor, $\boldsymbol{D}$, defined as:

$$D_{ij} = \frac{1}{2}\left(\frac{\partial V_i}{\partial x_j} + \frac{\partial V_j}{\partial x_i}\right) \tag{3}$$

is the sum of an elastic strain rate tensor $\boldsymbol{D}_e$ and a viscous strain rate tensor $\boldsymbol{D}_v$. The velocity vector, $\boldsymbol{V}$, is the fundamental unknown of our problem and all these entities are expressed in the fixed reference frame x_i. Now we decompose each strain rate tensor

$$\boldsymbol{D}_e = \frac{1}{3}tr(\boldsymbol{D}_e)\mathbf{I} + \hat{\boldsymbol{D}}_e \qquad \text{and} \qquad \boldsymbol{D}_v = \frac{1}{3}tr(\boldsymbol{D}_v)\mathbf{I} + \hat{\boldsymbol{D}}_v \tag{4}$$

where $\hat{\boldsymbol{D}}$ is the deviatoric part of $\boldsymbol{D}$ and $tr(\boldsymbol{D})$ represents the trace of the tensor.
Individually we express each deformation tensor as a function of the deviatoric stress tensor $\boldsymbol{\tau}$ and pressure p:

$$\frac{\overset{\nabla}{\boldsymbol{\tau}}}{2\mu} + \frac{\boldsymbol{\tau}}{2\eta} = \hat{\boldsymbol{D}}_e + \hat{\boldsymbol{D}}_v = \hat{\boldsymbol{D}} \tag{5}$$

where $\overset{\nabla}{\boldsymbol{\tau}}$ is the Jaumann corotational stress rate for an element of the continuum, μ is the shear modulus and η is shear viscosity. The isotropic part gives a scalar equation for the pressure:

$$\frac{\dot{p}}{K_e} + \frac{p}{\xi} = -tr(\boldsymbol{D}) \tag{6}$$

where K_e is the bulk modulus and ξ is the bulk viscosity. $\overset{\nabla}{p} \equiv \dot{p}$ as it p is a scalar.

$$\overset{\nabla}{\boldsymbol{\tau}} = \dot{\boldsymbol{\tau}} + \boldsymbol{\tau}\mathbf{W} - \mathbf{W}\boldsymbol{\tau} \tag{7}$$

where $\mathbf{W}$ is the material spin tensor,

$$W_{ij} = \frac{1}{2}\left(\frac{\partial V_i}{\partial x_j} - \frac{\partial V_j}{\partial x_i}\right) \tag{8}$$

The $\boldsymbol{W}$ terms account for material spin during advection which reorients the elastic stored-stress tensor.
We note that the form of equation (6) is unsuited to conventional fluids as the material has no long term resistance to compression. This behaviour is, however, relevant to the simulation of the coupled porous-flow, matrix deformation problem where it is common to ascribe an apparent bulk viscosity to the matrix material in order to model compaction effects on large scales (e.g. McKenzie 1984 [8]).

Numerical implementation

As we are interested in solutions where very large deformations may occur — including thermally driven fluid convection, we would like to work with a fluid-like system of equations. Hence we obtain a stress / strain-rate relation from (5) by expressing the Jaumann stress-rate in a difference form:

$$\overset{\nabla}{\boldsymbol{\tau}} \approx \frac{\boldsymbol{\tau}^{t+\Delta t} - \boldsymbol{\tau}^{t}}{\Delta t} - \mathbf{W}^{t}\boldsymbol{\tau}^{t} + \boldsymbol{\tau}^{t}\mathbf{W}^{t} \tag{9}$$

where the superscripts $t, t+\Delta t$ indicate values at the current and future timestep respectively. (5) and (6) become respectively

$$\boldsymbol{\tau}^{t+\Delta t} = \frac{\eta \Delta t}{\alpha + \Delta t}\hat{\boldsymbol{D}}^{t+\Delta t} + \frac{\alpha}{\alpha + \Delta t}\boldsymbol{\tau}^{t} + \frac{\alpha \Delta t}{\Delta t + \alpha}(\mathbf{W}^{t}\boldsymbol{\tau}^{t} - \boldsymbol{\tau}^{t}\mathbf{W}^{t}) \tag{10}$$

and

$$p^{t+\Delta t} = -\frac{\xi \Delta t}{\beta + \Delta t} D_{kk}^{t+\Delta t} + \frac{\beta}{\beta + \Delta t} p^{t} \tag{11}$$

where $\alpha = \eta/\mu$ is the shear relaxation time and $\beta = \xi/K_e$ is the bulk relaxation time. We can simplify the above equations by defining an effective viscosity η_{eff} and an effective compressibility ξ_{eff}:

$$\eta_{\text{eff}} = \eta \frac{\Delta t}{\Delta t + \alpha} \quad \text{and} \quad \xi_{\text{eff}} = \xi \frac{\Delta t}{\Delta t + \beta} \tag{12}$$

Then the deviatoric stress is given by

$$\boldsymbol{\tau}^{t+\Delta t} = \eta_{\text{eff}} \left(\hat{\boldsymbol{D}}^{t+\Delta t} + \frac{\boldsymbol{\tau}^{t}}{\mu \Delta t} + \frac{\mathbf{W}^{t}\boldsymbol{\tau}^{t}}{\mu} - \frac{\boldsymbol{\tau}^{t}\mathbf{W}^{t}}{\mu} \right) \tag{13}$$

and the pressure by

$$p^{t+\Delta t} = -\xi_{\text{eff}} \left(D_{kk}^{t+\Delta t} - \frac{p^{t}}{\Delta t K_e} \right) \tag{14}$$

To model an incompressible material K_e and ξ are made very large such that $D_{kk} \approx 0$.
Our system of equations is thus composed of a quasi-viscous part with modified material parameters and a right-hand-side term depending on values from the previous timestep. This approach minimizes the modification to the viscous flow code. Instead of using physical parameters for viscosity and bulk modulus, we use effective material properties (12) to take into account elasticity. During computation of the force term, we add elastic internal stresses from the previous timestep or from initial conditions.

$$F_i^{e,t} = \frac{\xi_{\text{eff}}}{K_e \Delta t} p_{,i}^{t-\Delta t} - \frac{\eta_{\text{eff}}}{\mu \Delta t} \sigma_{ij,j}^{t-\Delta t} \tag{15}$$

Computational method

Choice of Numerical Scheme

In fluid dynamics, where strains are generally very large, but not important in the constitutive relationship of the material, it is common to transform the equations to an Eulerian mesh and deal with convective terms explicitly. Problems arise whenever advection becomes strongly dominant over diffusion since an erroneous numerical diffusion dominates. In our case, the advection of material boundaries and the stress tensor are particularly susceptible to this numerical diffusion problem. Mesh-based Lagrangian formulations alleviate this difficulty, but at the expense of remeshing and the eventual development of a less-than optimal mesh configuration which increases complexity and can hinder highly efficient solution methods such as multigrid iteration.
A number of mesh-free alternatives are available: smooth particle hydrodynamics and discrete element methods are common examples from the fluid and solid mechanics fields respectively. These methods are extremely good at simulating the detailed behaviour of highly deforming materials with complicated geometries (e.g. free surfaces, fracture development), and highly dynamic systems. They are generally formulated to calculate explicitly interactions on a particle-particle scale which is usually impossible for creeping flow which has no inherent timescale for stress transfer. We have developed a hybrid approach – a particle in cell finite element method which uses a standard Eulerian finite element mesh (for fast, implicit solution) and a Lagrangian particle framework for carrying details of interfaces, the stress history etc.

The Particle in Cell Approach

Our method is based closely on the standard finite element method, and is a direct development of the material point method of Sulsky et al. (1995 [9]). The mesh is used to discretize the domain into elements, and the shape functions interpolate node points in the mesh in the usual fashion. The problem is formulated in a weak form to give an integral equation, and the shape function expansion produces a discrete (matrix) equation. Equation (1) in weak form, using the notation of (2) becomes

$$\int_\Omega N_{(i,j)}\tau_{ij}\,d\Omega - \int_\Omega N_{,i}p\,d\Omega = \int_\Omega N_i f_i\,d\Omega \tag{16}$$

where the trial functions, N, are the shape functions defined by the mesh, and we have assumed no non-zero traction boundary conditions are present. For the discretized problem, these integrals occur over subdomains (elements) and are calculated by summation over a finite number of sample points within each element. For example, in order to integrate a quantity, ϕ over the element domain Ω^e we replace the continuous integral by a summation

$$\int_{\Omega^e}\phi\,d\Omega \leftarrow \sum_p w_p\phi(\mathbf{x}_p) \tag{17}$$

In standard finite elements, the positions of the sample points, $\mathbf{x}_p$, and the weighting, w_p are optimized in advance. In our scheme, the $\mathbf{x}_p$'s correspond precisely to the Lagrangian points embedded in the fluid, and w_p must be recalculated at the end of a timestep for the new configuration of particles. Constraints on the values of w_p come from the need to integrate polynomials of a minimum degree related to the degree of the shape function interpolation, and the order of the underlying differential equation (e.g Hughes, 1987 [10]). These Lagrangian points carry the history variables which are therefore directly available for the element integrals without the need to interpolate from nodal points to fixed integration points. In our case, the distribution of particles is usually not ideal, and a unique solution for w_p cannot be found, or we may find we have negative weights which are not suitable for integrating physical history variables. We therefore store an initial set of w_p's based on a measure of local volume and adjust the weights slightly to improve the integration scheme. For more details and benchmarks, see Moresi et al. (2000 [11]).

Application to plate dynamics

Mathematical Model

We treat the Earth on a large scale as an incompressible, viscoelastic Maxwell fluid with infinite Prandtl number in which motions are driven by internal temperature variations. The force term from equation (1) is a gravitational body force due to density changes. We assume that these arise, for any given material, through temperature effects:

$$\nabla\cdot\boldsymbol{\tau} - \nabla p = g\rho_0(1-\alpha T)\hat{\mathbf{z}} \tag{18}$$

where g is the acceleration due to gravity, ρ_0 is material density at a reference temperature, α is the coefficient of thermal expansivity, and T is temperature. $\hat{\mathbf{z}}$ is a unit vector in the vertical direction. We have also assumed that the variation in density only needs to be considered in the driving term (the Boussinesq approximation).
The equation of motion is then

$$\nabla(\eta_{\rm eff}\mathbf{D}^{t+\Delta t}) - \nabla p = g\rho_0(1-\alpha T)\hat{\mathbf{z}} - \nabla\left(\eta_{\rm eff}\left[\frac{\boldsymbol{\tau}^t}{\mu\Delta t} + \frac{\mathbf{W}^t\boldsymbol{\tau}^t}{\mu} - \frac{\boldsymbol{\tau}^t\mathbf{W}^t}{\mu}\right]\right) \tag{19}$$

The velocity field $\mathbf{u}$ and pressure at $t+\Delta t$ can be solved for a given temperature distribution and the stress history from the previous step.
Motion is driven by the heat escaping from the interior. The energy equation governs the evolution of the temperature in response to diffusion of heat through the fluid. For a given element of fluid,

$$\frac{DT}{Dt} = -\kappa\nabla^2 T \tag{20}$$

where κ is the thermal diffusivity of the material.

Brittle failure

As we discussed above, plate models need to include a description of the brittle nature of the coldest part of the lithosphere. Here we use this term quite loosely to distinguish fault-dominated deformation which may result in seismic

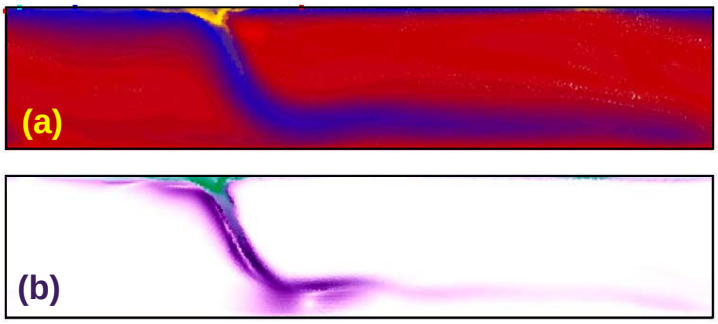

Figure 2: Example: snapshot from a convection simulation showing (a) the thermal field (and regions of yielding), and (b) the magnitude of the stored stresses

activity, from ductile creep which occurs at higher temperature and pressure. In all recent studies of mantle convection where the brittle lithospheric rheology has been taken into account, the brittle behaviour has been parameterized using a non-linear effective viscosity which is introduced whenever the stress would otherwise exceed the yield value $\tau_{\rm yield}$. This approach ignores details of individual faults, and treats only the influence of fault systems on the large-scale convective flow.
To determine the effective viscosity we extend (5) by introducing a von Mises plastic flow rule:

$$\frac{\overset{\nabla}{\boldsymbol{\tau}}}{2\mu} + \frac{\boldsymbol{\tau}}{2\eta} + \lambda\frac{\boldsymbol{\tau}}{2\left|\boldsymbol{\tau}\right|} = \hat{\boldsymbol{D}}_e + \hat{\boldsymbol{D}}_v + \hat{\boldsymbol{D}}_p = \hat{\boldsymbol{D}} \tag{21}$$

where λ is a parameter to be determined such that the stress remains on the yield surface, and $|\boldsymbol{\tau}| \equiv (\tau_{ij}\tau_{ij}/2)^{(1/2)}$. We again express the Jaumann stress rate in difference form (in the Lagrangian particle reference frame) to give:

$$\boldsymbol{\tau}^{t+\Delta t}\left[\frac{1}{2\mu\Delta t} + \frac{1}{2\eta} + \frac{\lambda}{2\left|\tau\right|}+\right] = \hat{\boldsymbol{D}}^{t+\Delta t} + \frac{1}{2\mu\Delta t}\boldsymbol{\tau}^t + \frac{1}{2\mu}(\mathbf{W}^t\boldsymbol{\tau}^t - \boldsymbol{\tau}^t\mathbf{W}^t) \tag{22}$$

No modification to the isotropic part of the problem is required when the von Mises yield criterion is used. At yield we use the fact that $|\boldsymbol{\tau}| = \tau_{\rm yield}$ to write

$$\boldsymbol{\tau}^{t+\Delta t} = \eta'\left[2\hat{\boldsymbol{D}}^{t+\Delta t} + \frac{1}{\mu\Delta t}\boldsymbol{\tau}^t + \frac{1}{\mu}(\mathbf{W}^t\boldsymbol{\tau}^t - \boldsymbol{\tau}^t\mathbf{W}^t)\right] \tag{23}$$

using an effective viscosity, η' given by

$$\eta' = \frac{\eta\tau_{\rm yield}\mu\Delta t}{\eta\tau_{\rm yield} + \tau_{\rm yield}\mu\Delta t + \lambda\eta\mu\Delta t} \tag{24}$$

We determine λ by equating the value of $|\boldsymbol{\tau}^{t+\Delta t}|$ with the yield stress in (23). Alternatively, in this particular case, we can obtain η' directly as

$$\eta' = \tau_{\rm yield}/\left|\hat{\mathbf{D}}_{\rm eff}\right| \tag{25}$$

where

$$\hat{\mathbf{D}}_{\rm eff} = 2\hat{\boldsymbol{D}}^{t+\Delta t} + \frac{1}{\mu\Delta t}\boldsymbol{\tau}^t + \frac{1}{\mu}(\mathbf{W}^t\boldsymbol{\tau}^t - \boldsymbol{\tau}^t\mathbf{W}^t) \tag{26}$$

and $|\boldsymbol{D}| = (2D_{ij}D_{ij})^{1/2}$.
The value of λ or η' is iterated to allow stress to redistribute from particles which become unloaded. The iteration is repeated until the velocity solution is unchanged to within the error tolerance required for the solution as a whole.

Plate modeling

Figure 2 shows a snapshot from a convection simululation which solves the full set of equations described above. The lithosphere has a viscosity contrast to the interior of a factor of 10^5, and the relaxation time is chosen to be comparable

to the time taken for material to be advected "around the bend" of the downwelling. The mobility of the lithosphere is possible because the yield stress is exceeded in a number of locations. During the evolution of the system the buoyancy forces, fluid convection and yielding in the lithosphere combine to produce a single downwelling, and a single spreading zone at the surface. However, the system is highly time-dependent and exhibits episodic behaviour in which bursts of subduction-like activity are interspersed with quiescent periods with almost stagnant lithosphere. The influence of elasticity is to produce a pronounced tendency for the downwellings to roll backwards. In purely viscous models the tendency is to roll forwards. Obviously, this model is very much simplified compared to the Earth — the lack of a third dimension, curvature, and continents are clearly deficiencies which need to be addressed. Fortunately, however, the introduction of these complicating details does not require any new algorithm development, only considerably greater computational resources.

Discussion

The algorithm described above is designed to introduce elastic effects into convection simulations where temperature-dependent viscosity and yielding dominate the mechanical behaviour. The viscosity of the mantle and the mantle lithosphere is very strongly dependent on temperature (several orders of magnitude variation over 1000 °C) whereas the shear modulus is not strongly affected (there is only a modest change in seismic wavespeed due to temperature). Therefore, elastic effects become unimportant outside the cold thermal boundary layer where viscosity is extremely large. The influence of elastic stresses is likely to be felt at the subduction zones where the lithosphere is bent into the interior of the Earth. In these regions stresses are typically close to the yield stress — a fact which allows the plates to move in the first place.

Our methodology is limited to a coarse continuum description of the subduction zone system at a resolution of a few km. This may be able to give us valuable information into the nature of plate tectonics, the thermal conditions in and around subducting lithosphere, and the stress state of the system. However, the resolution is too coarse to say anything about the detailed mechanics of the failure of lithospheric fault zones and the conditions for major failure to occur. For this we require a coupling of the large-scale code with an engineering-scale code (e.g. DEM or small-deformation Lagrangian FEM) using the large-scale to provide boundary conditions for the small scale. The issue of scale-bridging is important in many areas of numerical simulation. Essentially the same difficulties arise in material science where the atomic scale is best treated by molecular dynamics codes but the large scale must be treated as a continuum (e.g. Bernholc, 1999 [12]).

References

[1] Tackley, P. J., 1998, Self-consistent generation of tectonic plates in three dimensional mantle convection, Earth Planet. Sci. Lett., 157, 9-22.

[2] Tackley, P. J., 2000, The quest for self-consistent generation of plate tectonics in mantle convection models, AGU Monograph on The history and dynamics of global plate motions, ed. M. Richards, In Press.

[3] Moresi, L., Solomatov, V. S., 1998, Mantle convection with a brittle lithosphere: thoughts on the global tectonics styles of the Earth and Venus, Geophys. J. Int., 133, 669–682.

[4] Podlachikov, Yu., Yu., Lenardic, A., Yuen, D. A., Quareni, F., 1993, Dynamical consequences of stress focussing for different rheologies: Earth and Venus perspectives, EOS Trans. AGU, 74 no. 43/Suppl., 566.

[5] Melosh, H. J., 1978, Dynamic support of the outer rise, Geophys. Res. Lett., 5, 321–324.

[6] Gurnis, M., Eloy, C., Zhong, S., 1996, Free-surface formulation of mantle convection — II. Implications for subduction zone observables, Geophys. J. Int., 127, 719–727.

[7] Peltier, W. R., 1974, The impluse response of a Maxwell Earth, Rev. Geophys. Space Phys. 12, 649–669.

[8] McKenzie, D., 1984, The generation and compaction of partially molten rock, J. Petrology, 25, 713–765.

[9] Sulsky, D., Zhou, S.-J., Schreyer, H. L., 1995, Application of a particle-in-cell method to solid mechanics, Comput. Phys. Commun. 87, 236-252.

[10] Hughes, T. J.R., 1984, The Finite Element Method, Prentice-Hall.

[11] Moresi, L., Mühlhaus, H.-B., Dufour, F., Proceedings of the 5th International Workshop on Bifurcation and Localization in Geomechanics, Perth, W. A., Australia, Balkema.

[12] Bernholc, J., 1999, Computational materials science: The era of applied quantum mechanics, Physics Today, 52, No 9, 30–35.